

AUGUSTINOVIC, MARIO, M.S. Dasyscyphins F and G, New Drimane Meroterpenoids from a *Fitzroyomyces* Species (2020)
Directed by Dr. Nicholas H. Oberlies 24 pp.

As part of an ongoing investigation into the pharmaceutical potential of filamentous fungi, two new drimane meroterpenoids were discovered, which showed moderate cytotoxic activity across three cancer cell lines (MDA-MB-435, MDA-MB-231, OVCAR3). Compounds were isolated from a solid fermentation of *Fitzroyomyces* sp. (fungal strain MSX62440) and their structures were elucidated through NMR and HRESIMS data analysis. Absolute configuration was assigned through a combination of chiroptic and spectroscopic techniques in conjunction with predicted ECD calculations. Dasyscyphin G, previously published as a synthetic precursor to known compound dasyscyphin B, was also isolated as a natural product. Two compounds also showed activity against *B. anthracis*. Structure revision of dasyscyphin C was also performed based on ECD and NMR calculations.

DASYSCYPHINS F AND G, NEW DRIMANE MEROTERPENOIDS FROM A
FITZROYOMYCES SPECIES

by

Mario Augustinovic

A Thesis Submitted to
the Faculty of The Graduate School at
The University of North Carolina at Greensboro
in Partial Fulfillment
of the Requirements for the Degree
Master of Science

Greensboro
2020

Approved by

Committee Chair

Za moje roditelje, Jelica i Josip

APPROVAL PAGE

This thesis, written by Mario Augustinovic, has been approved by the following committee of the Faculty of The Graduate School at The University of North Carolina at Greensboro.

Committee Chair _____
Nicholas H. Oberlies

Committee Members _____
Mitchell P. Croatt

Daniel A. Todd

Date of Acceptance by Committee

Date of Final Oral Examination

ACKNOWLEDGEMENTS

First and foremost I wish to express my sincere appreciation to my advisor, Dr. Nicholas Oberlies. I am grateful for the four years I've spent under his mentorship and tutelage. His passion for science and innovation has been a constant source of inspiration for me.

I am also quite indebted to my committee members Dr. Mitchell Croatt and Dr. Daniel Todd. For Dr. Croatt, who taught me to challenge my ideas, which also drove me to join the Chemistry program as an undergraduate student. For Dr. Todd, who has spent immeasurable hours on both data analysis and banter, a combination of which I'm still impressed he can do so well.

I would also like to thank my first mentor, Dr. Noemi Paguigan, for the countless hours she spent training me. For my second mentor and best friend, Sonja Knowles, her ability to motivate and support others is unparalleled, and her approach to research is enviable.

I am eternally grateful to members of the Oberlies Group, who have always shown grace and support whenever needed, and humor more often than not. For Dr. Huzefa Raja, who taught me the value of believing in one's self. For Tyler Graf, who more than anyone showed me the value of hard work and resilience. For Dr. Laura Flores Bocanegra, I sincerely appreciate the NMR lessons and the constant laughs. Gratitude and praise must also be extended to Dr. Tamam El-Elimat, Dr. Jose Rivera-Chavez,

Kristof B. Cank, Allison Wright, Zuzu Faye, Zeinab Al-Subeh, Chris Roberts, and Robbie Shepherd.

Outside of the Oberlies Group, I'd also like to extend gratitude to Dr. Will Dodson, Israa Isawi, Robert Tikkanen, Daniel Ricks, Alysoun Gough, and Aidan Lytle. And finally, to my wife Laura, for her constant emotional support as I venture further into graduate studies.

TABLE OF CONTENTS

	Page
LIST OF FIGURES	vii
CHAPTER	
I. INTRODUCTION	1
II. RESULTS.....	5
III. METHODOLOGY	11
IV. CONCLUSIONS.....	15
REFERENCES	16
APPENDIX A. NMR SPECTRA	19

LIST OF FIGURES

	Page
Figure 1. Compounds Isolated from MSX62440.....	6
Figure 2. ECD Spectra of 1	8
Figure 3. Two Possible Structures of Dasyscyphin C.....	9
Figure 4. ECD Spectra of (A) 3a and (B) 3b	9
Figure 5. ^1H and ^{13}C NMR Spectra of 1	19
Figure 6. COSY NMR Spectrum of 1	20
Figure 7. HSQC NMR Spectrum of 1	21
Figure 8. HMBC NMR Spectrum of 1	22
Figure 9. ^1H and ^{13}C NMR Spectra of 2	23
Figure 10. ^1H and ^{13}C NMR Spectra of 3	24

CHAPTER I

INTRODUCTION

Cancer is the second leading cause of death in the world with a mortality rate of about 1 in 6 incidences. Breast cancer is considered the leading diagnosed type in women, with over 25% of all cases and over 600,000 deaths in 2018.¹ The ability for multiple variations to exist within one type of cancer can make treatment options difficult.² Combinational methods to treat cancer include radiation therapy, immunotherapy, chemotherapeutic agents, and surgeries.³ Chemotherapeutic agents have been not only been synthesized by advances in combinational chemistry but also through the discovery of said agents in nature.⁴ These natural products are secondary metabolites produced by organisms, in part to defend themselves from other organisms but also to help facilitate reproduction. Since nature is able to produce such complex structures with defined stereospecific cores, natural products are often an excellent source of drugs.⁵⁻⁶ Some drugs like taxol have translated directly to the clinic, while others have taken extraordinary steps in the realm of combinational synthetic chemistry to become drugs.⁷⁻⁸

Bioactivity guided fractionation is a systematic approach to the separation of biologically active natural products from their non-active components.⁹ The process entails a series of chromatographic steps and biological screenings to ensure the discovery of such molecules. The extract of an organism of choice is obtained first through a series of extraction techniques which ultimately lead to a crude organic mass.

Normal phase chromatography employs a polar stationary phase like silica with a nonpolar mobile phase like chloroform or hexanes.¹⁰ In contrast, reverse phase chromatography uses a nonpolar stationary phase like C₁₈ bound silica with polar solvents like acetonitrile and water.¹¹ This material is then separated using either normal phase flash or column chromatography to distinguish the material into defined sections of polarity.¹² The original extract as well as its constituents are then tested against a bioassay of choice, which will designate which fractions are worth continuing to resolve. At this point, active fractions can be separated with either normal phase or reverse phase techniques, depending on the polarity of the components in the mixture. Both types of chromatography are generally used to expose the fraction of interest to a wide variety of solvent combinations to best optimize the separation into pure compounds. After separation is achieved, the compounds are then analyzed by a series of spectroscopic and spectrometric methods to resolve the structure. Final biological screenings are also collected at this point to discern which component of the mixture was active. At this point, other bioactivities can also be profiled based on different biological screenings.

Natural products often contain multiple stereocenters that cause the structure elucidation of said molecules to be difficult. One dimensional (nuclear magnetic resonance) experiments are often enough for the assignment of planar structure of molecules, however stereo-enriched compounds are often difficult to deduce even with two-dimensional experiments like HMBC¹³ (heteronuclear multiple bond correlation spectroscopy) or COSY (correlation spectroscopy). Both of these techniques rely on “through bond” correlations that allow for the chemist to associate the hydrogen of

choice's environment. However, these experiments do not take into consideration those interactions that happen "through space," which is where the NOESY (nuclear Overhauser effect spectroscopy) experiment becomes relevant. NOESY¹⁴, which does not rely on proximity between atoms to be observed, is an experiment that allows for "through space" interactions. Correlations from the COSY experiment can also be observed in the NOESY experiment, since "through space" interactions do not have to but can include "through bond" interactions. However, with the use of the NOESY experiment alone, only relative configuration can be assigned.¹⁵ This is because when a structure is assigned through NOESY correlations, the absolute configurations be the structure proposed or its enantiomer. This is where a technique like circular dichroism can come into play.

Circular dichroism spectroscopy is a method that involves the application of circularly polarized light to molecules of interest.¹⁶ An orthogonal method called ECD (electronic circular dichroism) measures the absorption of the UV region. As circularly polarized light is applied to the molecule of interest, it will rotate in a defined way and absorb light at a particular wavelength.¹⁷⁻¹⁹

Computational chemistry has made great strides in the development of simulation technology capable of modeling the chemical environments of structures.²⁰ One area in particular is in the ability to use TD-DFT (time dependent density functional theory) calculations to investigate the spectroscopic properties of small molecules.²¹⁻²² Structures can be modelled first through the use of the NOESY NMR experiment, which assigns the relative configuration of a molecule of interest. Then, if one models the structure to

calculate first its minimal energy conformation and then its ECD profile, one is able to assign the absolute configuration of a molecule.²³⁻²⁵

CHAPTER II

RESULTS

The presented study focuses on fungal strain MSX62440 and its associated isolated compounds. The compounds isolated in MSX62440 belong to a small family of meroterpenoids called the dasyscyphins, of which there are currently five published in the literature.²⁶⁻²⁸ These meroterpenoids are the product MSX62440 was described as a *Fitzroyomyces* sp., and dasyscyphins F-H represent three new meroterpenoids, which are a combination isoprene biosynthesis and polyketide biosynthesis.²⁹ Also isolated was dasyscyphin C, which showed irregularities within the original structure assignment of the molecule. The issues are described in the chemical description of dasyscyphin C, where both NMR and ECD calculations are used. Bioactivity guided fractionation was utilized for the separation of said molecules, and activities in cell cytotoxicity assays and antimicrobial screenings are noted. Of particular interest in the activity against *B. anthracis*, of which **3** show particular activity against.

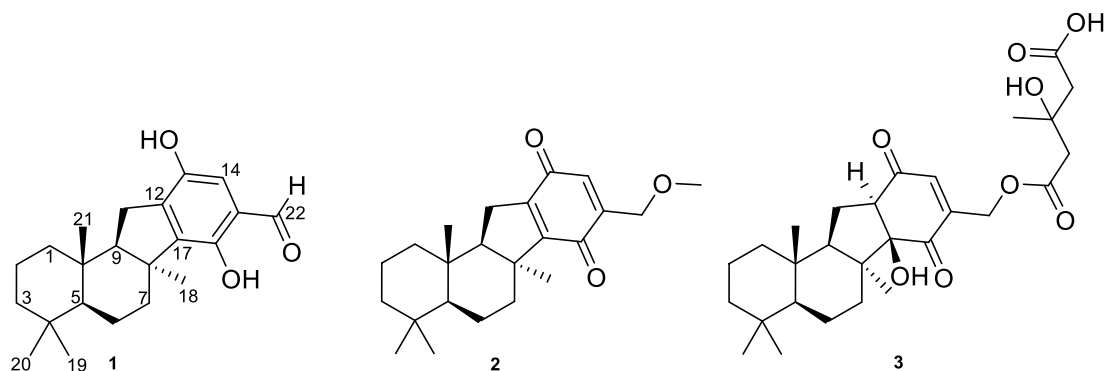


Figure 1. Compounds Isolated from MSX62440

Dasyscyphin F (2.93 mg) (**1**) was isolated as an optically active ($[\alpha]_D^{20} = +17^\circ$) yellow powder and a molecular formula was established as $C_{22}H_{30}O_3$ by HRESIMS (m/z $[M+H]^+$ 343.2257, calculated for $C_{22}H_{31}O_3^+$ 343.2268, -3.1 ppm), indicating index of hydrogen deficiency of 8. Analysis of the 1H and ^{13}C NMR data indicated the presence of 22 carbon atoms, consisting of four methyl groups, six methylene groups, and four methine groups (one aromatic, one aldehydic, two aliphatic). Three of the eight remaining carbons were determined to be oxygenated (one chelated and one hydroxyl) as well as one carbonyl group. Relative configuration was assigned through NOESY correlations, and TDDFT calculations allowed for the assignment of absolute configuration through circular dichroism.

Extensive 1H - ^{13}C HMBC spectrum analysis revealed two partial structures, subunits a and b, of **1**. Unit a (2,5 dihydroxy-benzaldehyde moiety), was identified as a 1,2,4,5,6-pentasubstituted aromatic ring based on the singlet resonance at δ_H 6.75 (H-14) and ^{13}C NMR shifts (δ_C 140.1, 153.0, 116.8, 120.1, 144.6, 142.0) observed for C-12, C-

13, C-14, C-15, C-16, C-17, respectively. Furthermore, HMBC correlations from H-22 ($\delta_{\text{H}} 9.75$) to C-12 and C-14 indicated an aldehyde directly bound to the aromatic system. Finally, a resonance at $\delta_{\text{H}} 10.82$ showed correlations with C-12/C-13/C-14, indicating its position to be at C-13, along with a resonance at $\delta_{\text{C}} 153.0$, typical for a phenolic carbon. Subunit a accounted for five indices of hydrogen deficiency, leaving a total of three for subunit b.

Due to the lack of olefins in the ^1H and ^{13}C NMR data, subunit b would need to contain three aliphatic rings to satisfy the index of hydrogen deficiency. Subunit b contained four methyl groups and highly saturated ring system, with overlaying methylene groups. HSQC confirmed the presence of only three resonances that accounted for quaternary carbons ($\delta_{\text{C}} 33.4/\text{C-4}$, $37.3/\text{C-10}$, $48.5/\text{C-8}$), indicating a pair of inequivalent geminal dimethyl groups. A fourth quaternary carbon would otherwise need to be present since the methyl groups are all singlets. ^1H - ^{13}C HMBC data indicated that the C-11 methylene group ($\delta_{\text{C}} 29.4$, $\delta_{\text{H}} 2.90$ dd, 2.73 d) has multiple correlations with the aromatic ring ($\delta_{\text{C}} \text{C-12, C-16, C-17}$), and the aromatic proton also correlates with C-11, indicating a methylene group alpha to the aromatic ring system. C-11 also contains two inequivalent protons, of which one splits with its pair ($\delta_{\text{H}} 2.73\text{-}2.90$ where $J_{\text{H-H}}=17.7$) while the other splits with its pair and a tertiary proton ($\delta_{\text{H}} 2.90\text{-}2.73$, $2.90\text{-}1.75$ $J_{\text{H-H}}=8.0$) with a resonance of $\delta_{\text{C}} 62.0$. Compound 1's remaining ^{13}C and ^1H spectra resembled that of the terpenoid moiety with the dasyscyphins. Electronic circular dichroism was also used for the assignment of absolute configuration, which was only possible after the assignment of relative configuration using NOESY correlations.

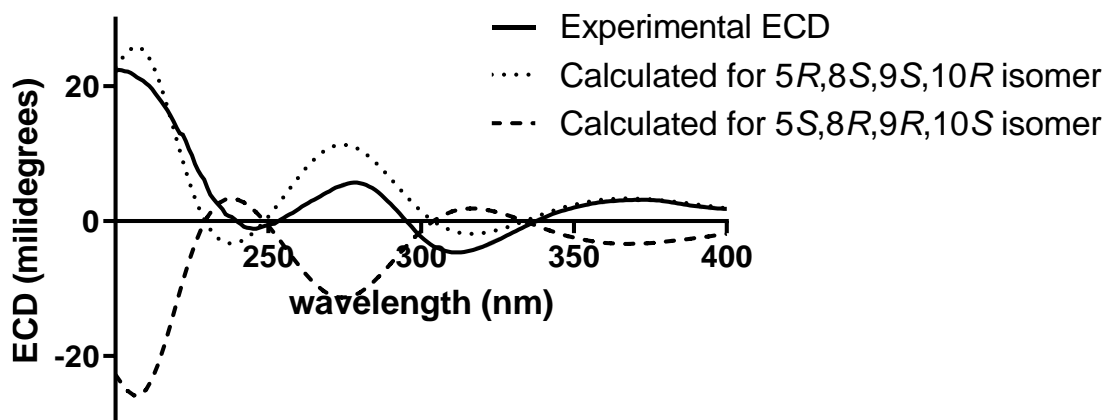


Figure 2. ECD Spectra of **1**

Dasyscyphin G (**2**), previously reported as a synthetic intermediate, was also isolated and characterized.²⁶ Its NMR data was consistent with literature data. It showed little to no activity and was assigned the trivial name Dasyscyphin G. **2** also decomposed before the ability to collect further chiroptic data.

Dasyscyphin C (**3**) showed previous activity in various antibiotic and cancer cell lines. NMR data was consistent with the literature, but ¹³C NMR data seemed disputable due to two shifts at 196.0 ppm and 202.4 ppm, which was originally reported as a 1,2 dione moiety. However, both shifts seem to represent similar chemical environments, which would be inconsistent with the original structure proposed.³⁰⁻³¹ Instead, a 1,4 dione moiety would be more representative of the data at hand. While a crystal was prepared, both ECD and NMR calculations³² were performed on the proposed (literature) structure as well as the suggested structure based on structure revision. Both a published and proposed version of dasyscyphin C were modelled and energy minimized before ECD

and NMR calculations were performed. Below indicate the results of ECD and NMR calculations.

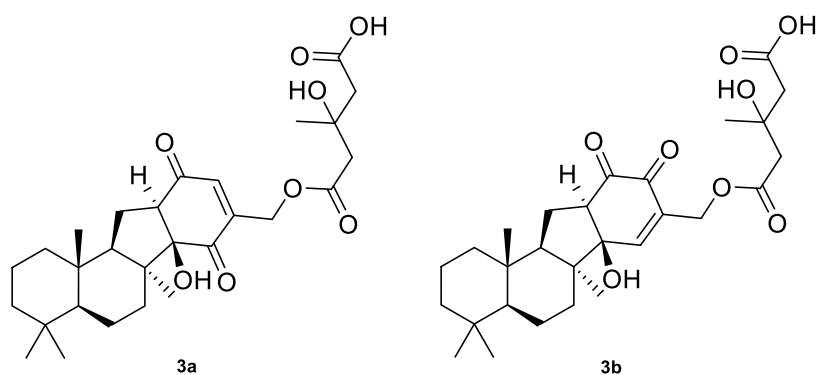


Figure 3. Two Possible Structures of Dasyscyphin C

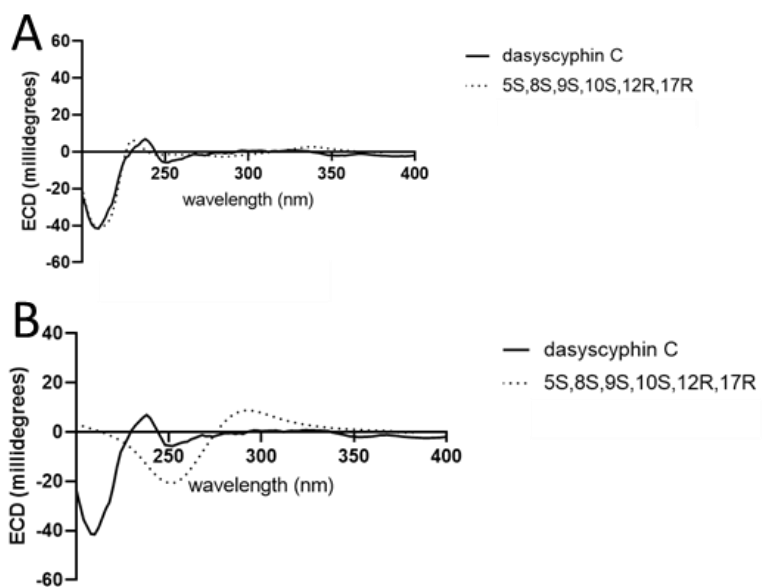


Figure 4. ECD Spectra of (A) 3a and (B) 3b

Calculated ECD spectra were created from modelling both structures (3a and 3b) of dasyscyphin C, and show a clear discrepancy between the 3a and 3b. In particular, the experimental data matches strongly with revised structure 3a instead of 3b, and 3b shows a marginally different ECD profile.

As represented (Fig. 5), 3a's calculated and experimented CD spectra match much more similarly than that of 3b's calculated and experimental CD spectra. This variation in calculated CD spectra is a result of the change of the 1,2 dione core to the 1,4 dione core, which causes the chromophore in question to elicit a new set of Cotton effects. The experimental Cotton Effects at 210 and 245 match the calculated 3a almost exactly but 3b's experimental data is much less similar and shows that the modelled structure does not match the experimental data. NMR ¹³C calculations were also performed, and the data is presented as a table shown below.

Calculated carbon data are increasingly used for the verification of assigned structures, whether through elucidation or revision.³³⁻³⁵ The data shows that the modelled structure 3a more closely matches the experimental data than 3b does, which is the originally published structure.^{27, 36} This data, along with calculated ECD spectra, suggests that the original structure was incorrectly assigned as 1,2 dione and dasyscyphin C should in fact be corrected to a 1,4 dione.

Compounds **1-3** were tested against three human tumor cell lines. **1** and **3** were moderately active in the screening (with IC₅₀ values ranging between 4 and 16 μM against all cell lines) compared to taxol as the control (ranging between 2 and 7 nM). Compounds **1** and **3** were also tested for antimicrobial activity, of which **3** showed moderate activity against *Bacillus anthracis* in particular (with MIC value of 2.0 μg/mL), which was previously unreported.

CHAPTER III

METHODOLOGY

Optical rotations, UV, and IR data were measured using a Rudolph Research Autopol III polarimeter (Rudolph Research Analytical), a Varian Cary 100 Bio UV-Vis spectrophotometer (Varian Inc.) and a Perkin-Elmer Spectrum One with Universal ATR attachment (PerkinElmer). NMR spectra were recorded using a JEOL ECA-500 NMR spectrometer operating at 500 MHz for ^1H and 125 MHz or a JEOL ECS-400 NMR spectrometer operating at 400 MHz for ^1H and 100 MHz for ^{13}C and equipped with a high sensitivity JEOL Royal probe and a 24-slot autosampler (JEOL Ltd). Residual solvent signals were utilized for referencing. HRMS data were collected using a Thermo LTQ Orbitrap XL mass spectrometer equipped with an electrospray ionization source (Thermo Fisher Scientific). A Waters Acquity UPLC System (Waters Corp.) utilizing a Waters BEH C_{18} column (1.7 μm ; 50 \times 2.1 mm) and analyzed using the software XCalibur. A Varian ProStar HPLC system equipped with ProStar 210 pumps, a ProStar 335 Photodiode array detector (PDA), and Galaxie Chromatography Workstation software (version 1.9.3.2, Varian Inc.) was used for data collection and analysis. Flash chromatography was conducted on a Teledyne Isco CombiFlash Rf 200 system using RediSep RF Gold HP Silica columns (both from Teledyne Isco) that was coupled with UV and evaporative light-scattering detectors

(ELSD). All other reagents and solvents were obtained from Fisher Scientific and were used without further purification.

Phylogram of the most likely tree ($-\ln L = 5786.07$) from a RAxML analysis of 26 strains based on ITS region sequence data (1020 bp). Numbers refer to RAxML bootstrap support values $\geq 70\%$ based on 1000 replicates. Strain MSX62440 is identified as *Fitzroyomyces* sp., Ostropales, Stictidaceae, Lacanoromycetes, Ascomycota as it groups with isolates of *Fitzroyomyces cyperacearum*. It is also forms a clade with *Neofitzroyomyces nerii* sharing 100% RAxML bootstrap support. MSX62440 is highlighted in a brown box. Three-week-old culture on potato dextrose agar is shown. Bar indicates nucleotide substitutions per site. The tree is rooted with members of Trapeliaceae Baeomycetales. Taxon sampling was performed following a recent taxonomic study by Yang et al.³⁷⁻³⁸

Briefly, cultures of strain MSX62440 were grown in one 2.8-L Fernbach flask (Corning, Inc., Corning, NY, USA) containing 150 g rice and 300 mL H₂O. A seed culture grown in YESD medium was used as the inoculum. Following incubation at 22 °C for 14 days, to the solid fermentation culture of MSX62440, 100 mL of acetone was added and chopped, and the resulting mixture sat for 15 minutes. The slurry was filtered under vacuum and an additional 100 mL acetone was added. The filtrate was then filtered through silica on a 250 mL glass fritted funnel. The de-sugared extract was then dried *in vacuo* and reconstituted in 200 mL of ethyl acetate and 200 mL of H₂O, and transferred to a separatory funnel. The aqueous layer was drawn off, and set aside. The organic layer

was drawn off and dried off *in vacuo*. The aqueous layer was repartitioned with an additional 100 mL of ethyl acetate, then this process was repeated twice to pull any remaining organic material from the aqueous layer. The organic was dried down *in vacuo* and repartitioned in 100 mL of 1:1 MeOH-MeCN and 100 mL of hexane, and then partitioned in a separatory funnel. The MeOH-MeCN layer was collected and concentrated *in vacuo*. The resulting MeOH-MeCN extract was then adsorbed on Celite 545 (Acros Organics) and fractionated via flash chromatography on a 4g RediSep Rf Gold Si-gel column using a gradient solvent system of hexane-CHCl₃-MeOH at a flow rate of 18 mL/min over 90 column volumes for a duration of 24.0 min. Fractions were collected every 9.0 mL and pooled according to the UV and ELSD profiles, which resulted in five combined fractions in total (F_I-F_V). F_{III} was subjected to two rounds of preparative HPLC using a gradient system of 90 to 100 CH₃CN-H₂O (0.1% formic acid) over 30 minutes at a flow rate of 17 mL/min and T3 column to yield dasyscyphin F (T_R=18.2 minutes) and dasyscyphin G (T_R=25.5 minutes). A separate sample preparation resulted in seven fractions in total (F_I-F_{VII}). F_{II} was subjected to one round of preparative HPLC using a gradient system of 87 to 100 CH₃CN-H₂O (0.1% formic acid) over 30 minutes at a flow rate of 17 mL/min and T3 column to yield **3** (T_R=12 minutes)

The TDDFT calculations, such as NMR and circular dichroism, were performed as previously described using the Gaussian'16 program package.³⁹ A 3D model of dasyscyphin F and dasyscyphin C were built and geometry optimized using Spartan'10 software (www.wavefunction.com). The resulting conformers were filtered, checked for

duplicity, and minimized using a DFT force field at the B3LYP/6-311+G(2d,p) level of theory. Conformational analysis was performed by a Monte Carlo search protocol as implemented in the same software under the semiempirical method (PM3). ECD calculations using the self-consistent reaction field with conductor-like continuum solvent model in MeOH were subsequently performed on the obtained DFT-minimized major conformers of both 5R,8S,9S,10R and 5S,8R,9R,10S enantiomers of dasyscyphin F at the B3LYP/G-31+G(d,p) level of theory. ECD calculations using the self-consistent reaction field with conductor-like continuum solvent model in MeOH were also subsequently performed on the obtained DFT-minimized major conformers of both 5S,8S,9S,10S,12R,17R and 5R,8R,9R,10R,12S,17S enantiomers of dasyscyphin C at the B3LYP/G-31+G(d,p) level of theory. Subsequently, the excitation energy (nm) and rotatory strength (R) in dipole velocity (Rvel) and dipole length (Rlen) forms obtained from the calculations were then used to simulate the ECD curves. A 3D model of dasyscyphin C was generated and geometry optimized using Schrodinger Suite under Maestro (source) and conformational searches were performed using Schrodinger Suite's MacroModel. The resulting conformers were filtered, checked for duplicity, and minimized using a DFT force field at the M062X/6-31+G(d,p) level of theory. NMR shielding constants were calculated with the GIAO method at B3LYP/6-311+G(2d,p) level of theory with the IEFPCM model in chloroform solvent. The obtained shielding constants were converted to chemical shifts by referencing TMS at 0 ppm.⁴⁰

CHAPTER IV

CONCLUSIONS

In summary, initial bioassay guided fraction of fungal strain MSX62440 led to the isolation of three new drimane sesquiterpenoids. The initial screening tested against three cancer cell lines: MDA-MB-435 (melanoma), MDA-MB-231 (breast) and OVCAR3 (Ovarian). Further fractionation allowed for the isolation of compounds **1** and **2**, while regrowth of MSX62440 allowed for the isolation of **3** and **4**. Extensive 1D and 2D NMR data analysis allowed for the assignment of the planar structure of **1-4**. While **2** degraded before further data could be collected, compounds **1**, **3**, and **4** all had absolute configuration assigned through a combination of 2D NMR experiments and chiroptic techniques. In particular, the calculation of electronic circular dichroism spectra allowed for the comparison of enantiomers that were assigned relatively through NOESY correlations. The dasyscyphins are low in number in the literature, but are structurally unique and complex with interesting bioactivities. Preliminary gene sequencing placed MSX62440 as a member of the *Fitzroyomyces* sp., which is a member of the *Lecanoromycetes*, which represent lichenized fungi as well as saprobes and endophytes. Structure revision of **4** was performed by calculation of ^{13}C chemical shifts and ECD predictions.

REFERENCES

1. Siegel, R. L.; Miller, K. D.; Jemal, A., Cancer statistics, 2019. *CA: a cancer journal for clinicians* **2019**.
2. Aysola, K.; Desai, A.; Welch, C.; Xu, J.; Qin, Y.; Reddy, V.; Matthews, R.; Owens, C.; Okoli, J.; Beech, D. J., Triple negative breast cancer—an overview. *Hereditary genetics: current research* **2013**, *2013* (Suppl 2).
3. Baskar, R.; Lee, K. A.; Yeo, R.; Yeoh, K.-W., Cancer and radiation therapy: current advances and future directions. *International journal of medical sciences* **2012**, *9* (3), 193.
4. Wani, M. C.; Taylor, H. L.; Wall, M. E.; Coggon, P.; McPhail, A. T., Plant antitumor agents. VI. Isolation and structure of taxol, a novel antileukemic and antitumor agent from *Taxus brevifolia*. *Journal of the American Chemical Society* **1971**, *93* (9), 2325-2327.
5. Cragg, G. M.; Grothaus, P. G.; Newman, D. J., Impact of natural products on developing new anti-cancer agents. *Chemical reviews* **2009**, *109* (7), 3012-3043.
6. Mann, J., Natural products in cancer chemotherapy: past, present and future. *Nature Reviews Cancer* **2002**, *2* (2), 143-148.
7. Hanada, M.; SUGAWARA, K.; KANETA, K.; TODA, S.; NISHIYAMA, Y.; TOMITA, K.; YAMAMOTO, H.; KONISHI, M.; OKI, T., Epoxomicin, a new antitumor agent of microbial origin. *The Journal of antibiotics* **1992**, *45* (11), 1746-1752.
8. Kim, K. B.; Crews, C. M., From epoxomicin to carfilzomib: chemistry, biology, and medical outcomes. *Natural product reports* **2013**, *30* (5), 600-604.
9. Ballschmiter, K.; Wößner, M., Recent developments in adsorption liquid chromatography (NP-HPLC) A review. *Fresenius' journal of analytical chemistry* **1998**, *361* (8), 743-755.
10. Kirkland, J.; Dilks Jr, C.; DeStefano, J., Normal-phase high-performance liquid chromatography with highly purified porous silica microspheres. *Journal of Chromatography A* **1993**, *635* (1), 19-30.
11. Kingston, D. G., High performance liquid chromatography of natural products. *Journal of Natural Products* **1979**, *42* (3), 237-260.
12. Dorsey, J. G.; Dill, K. A., The molecular mechanism of retention in reversed-phase liquid chromatography. *Chemical Reviews* **1989**, *89* (2), 331-346.
13. Furrer, J., A comprehensive discussion of HMBC pulse sequences, part 1: the classical HMBC. *Concepts in Magnetic Resonance Part A* **2012**, *40* (3), 101-127.
14. Reggelin, M.; Hoffmann, H.; Koeck, M.; Mierke, D. F., Determination of conformation and relative configuration of a small, rapidly tumbling molecule in solution by combined application of NOESY and restrained MD calculations. *Journal of the American Chemical Society* **1992**, *114* (9), 3272-3277.

15. Andersson, T.; Berova, N.; Nakanishi, K.; Carter, G. T., Relative and absolute configurations of ganefromycin α . *Organic letters* **2000**, 2 (7), 919-922.
16. Stephens, P. J.; Harada, N., ECD cotton effect approximated by the Gaussian curve and other methods. *Chirality: The Pharmacological, Biological, and Chemical Consequences of Molecular Asymmetry* **2010**, 22 (2), 229-233.
17. Berova, N.; Di Bari, L.; Pescitelli, G., Application of electronic circular dichroism in configurational and conformational analysis of organic compounds. *Chemical Society Reviews* **2007**, 36 (6), 914-931.
18. Pescitelli, G.; Di Bari, L.; Berova, N., Conformational aspects in the studies of organic compounds by electronic circular dichroism. *Chemical Society Reviews* **2011**, 40 (9), 4603-4625.
19. Diedrich, C.; Grimme, S., Systematic investigation of modern quantum chemical methods to predict electronic circular dichroism spectra. *The Journal of Physical Chemistry A* **2003**, 107 (14), 2524-2539.
20. Ramalingam, S.; Karabacak, M.; Periandy, S.; Puviarasan, N.; Tanuja, D., Spectroscopic (infrared, Raman, UV and NMR) analysis, Gaussian hybrid computational investigation (MEP maps/HOMO and LUMO) on cyclohexanone oxime. *Spectrochimica Acta Part A: Molecular and Biomolecular Spectroscopy* **2012**, 96, 207-220.
21. Li, X.-C.; Ferreira, D.; Ding, Y., Determination of absolute configuration of natural products: theoretical calculation of electronic circular dichroism as a tool. *Current organic chemistry* **2010**, 14 (16), 1678-1697.
22. Pinto, B. N.; Teixeira, M. G.; Alvarenga, E. S., Synthesis and structural elucidation of a phthalide analog using NMR analysis and DFT calculations. *Magnetic Resonance in Chemistry* **2020**.
23. Bruhn, T.; Schaumlöffel, A.; Hemberger, Y.; Bringmann, G., SpecDis: Quantifying the comparison of calculated and experimental electronic circular dichroism spectra. *Chirality* **2013**, 25 (4), 243-249.
24. Li, H.; Sun, W.; Deng, M.; Qi, C.; Chen, C.; Zhu, H.; Luo, Z.; Wang, J.; Xue, Y.; Zhang, Y., Aspersins A and B, two novel meroterpenoids with an unusual 5/6/6/6 ring from the marine-derived fungus *Aspergillus versicolor*. *Marine drugs* **2018**, 16 (6), 177.
25. Neuhaus, G. F.; Adpressa, D. A.; Bruhn, T.; Loesgen, S., Polyketides from Marine-Derived *Aspergillus porosus*: Challenges and Opportunities for Determining Absolute Configuration. *Journal of natural products* **2019**, 82 (10), 2780-2789.
26. Akhaouzan, A.; Fernandez, A.; Mansour, A. I.; Alvarez, E.; Haidoeur, A.; Alvarez-Manzaneda, R.; Chahboun, R.; Alvarez-Manzaneda, E., First synthesis of antitumoral dasyscyphin B. *Organic & biomolecular chemistry* **2013**, 11 (36), 6176-6185.
27. Mierau, V.; de La Parra, V. R.; Sterner, O.; Anke, T., The Dasyscyphins A~C and Niveulone, New Biologically Active Compounds from the Ascomycete *Dasyscyphus niveus*. *The Journal of antibiotics* **2006**, 59 (1), 53.
28. Zhang, L.; Xie, X.; Liu, J.; Qi, J.; Ma, D.; She, X., Concise total synthesis of (\pm)-dasyscyphin D. *Organic letters* **2011**, 13 (11), 2956-2958.
29. Schmidt-Dannert, C., Biosynthesis of terpenoid natural products in fungi. In *Biotechnology of Isoprenoids*, Springer: 2014; pp 19-61.

30. Peng, Y.; Ni, S.-J.; Li, J.; Li, M.-Y., Three new dolabrane diterpenes from the Chinese mangrove plant of *Ceriops tagal*. *Phytochemistry Letters* **2017**, *21*, 38-41.
31. Sassa, T.; Ishizaki, A.; Nukina, M.; Ikeda, M.; Sugiyama, T., Isolation and identification of new antifungal macrophorins E, F and G as malonyl meroterpenes from *Botryosphaeria berengeriana*. *Bioscience, biotechnology, and biochemistry* **1998**, *62* (11), 2260-2262.
32. Krivdin, L. B., Computational protocols for calculating ¹³C NMR chemical shifts. *Progress in nuclear magnetic resonance spectroscopy* **2019**.
33. Rychnovsky, S. D., Predicting NMR spectra by computational methods: Structure revision of hexacyclinol. *Organic letters* **2006**, *8* (13), 2895-2898.
34. Barone, G.; Gomez-Paloma, L.; Duca, D.; Silvestri, A.; Riccio, R.; Bifulco, G., Structure validation of natural products by quantum-mechanical GIAO calculations of ¹³C NMR chemical shifts. *Chemistry—A European Journal* **2002**, *8* (14), 3233-3239.
35. Yang, X.-W.; Grossman, R. B., Revision of the Structure of Hypatulone A by NMR, Computations, and Biosynthetic Considerations. *Organic Letters* **2020**.
36. de la Parra, V. R.; Mierau, V.; Anke, T.; Sterner, O., Cytotoxic terpenoids from *Dasyscyphus niveus*. *Tetrahedron* **2006**, *62* (8), 1828-1832.
37. Yang, C.; Baral, H.-O.; Xu, X.; Liu, Y., *Parakarstenia phyllostachydis*, a new genus and species of non-lichenized Odontotremataceae (Ostropales, Ascomycota). *Mycol Prog* **2019**, *18* (6), 833-845.
38. Raja, H. A.; Miller, A. N.; Pearce, C. J.; Oberlies, N. H., Fungal identification using molecular tools: a primer for the natural products research community. *Journal of natural products* **2017**, *80* (3), 756-770.
39. Frisch, M. J.; Trucks, G. W.; Schlegel, H. B.; Scuseria, G. E.; Robb, M. A.; Cheeseman, J. R.; Scalmani, G.; Barone, V.; Petersson, G. A.; Nakatsuji, H.; Li, X.; Caricato, M.; Marenich, A. V.; Bloino, J.; Janesko, B. G.; Gomperts, R.; Mennucci, B.; Hratchian, H. P.; Ortiz, J. V.; Izmaylov, A. F.; Sonnenberg, J. L.; Williams; Ding, F.; Lipparini, F.; Egidi, F.; Goings, J.; Peng, B.; Petrone, A.; Henderson, T.; Ranasinghe, D.; Zakrzewski, V. G.; Gao, J.; Rega, N.; Zheng, G.; Liang, W.; Hada, M.; Ehara, M.; Toyota, K.; Fukuda, R.; Hasegawa, J.; Ishida, M.; Nakajima, T.; Honda, Y.; Kitao, O.; Nakai, H.; Vreven, T.; Throssell, K.; Montgomery Jr., J. A.; Peralta, J. E.; Ogliaro, F.; Bearpark, M. J.; Heyd, J. J.; Brothers, E. N.; Kudin, K. N.; Staroverov, V. N.; Keith, T. A.; Kobayashi, R.; Normand, J.; Raghavachari, K.; Rendell, A. P.; Burant, J. C.; Iyengar, S. S.; Tomasi, J.; Cossi, M.; Millam, J. M.; Klene, M.; Adamo, C.; Cammi, R.; Ochterski, J. W.; Martin, R. L.; Morokuma, K.; Farkas, O.; Foresman, J. B.; Fox, D. J. *Gaussian 16 Rev. C.01*, Wallingford, CT, 2016.
40. Willoughby, P. H.; Jansma, M. J.; Hoye, T. R., A guide to small-molecule structure assignment through computation of (¹H and ¹³C) NMR chemical shifts. *Nature protocols* **2014**, *9* (3), 643.

APPENDIX A
NMR SPECTRA

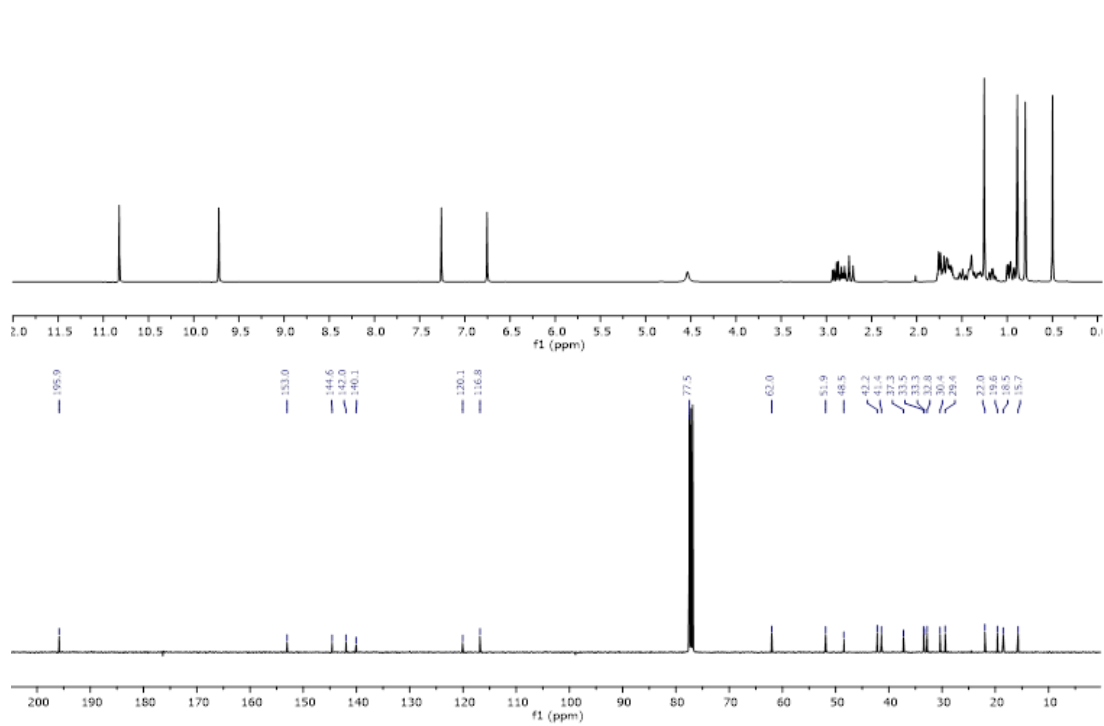


Figure 5. ^1H and ^{13}C NMR Spectra of **1**.

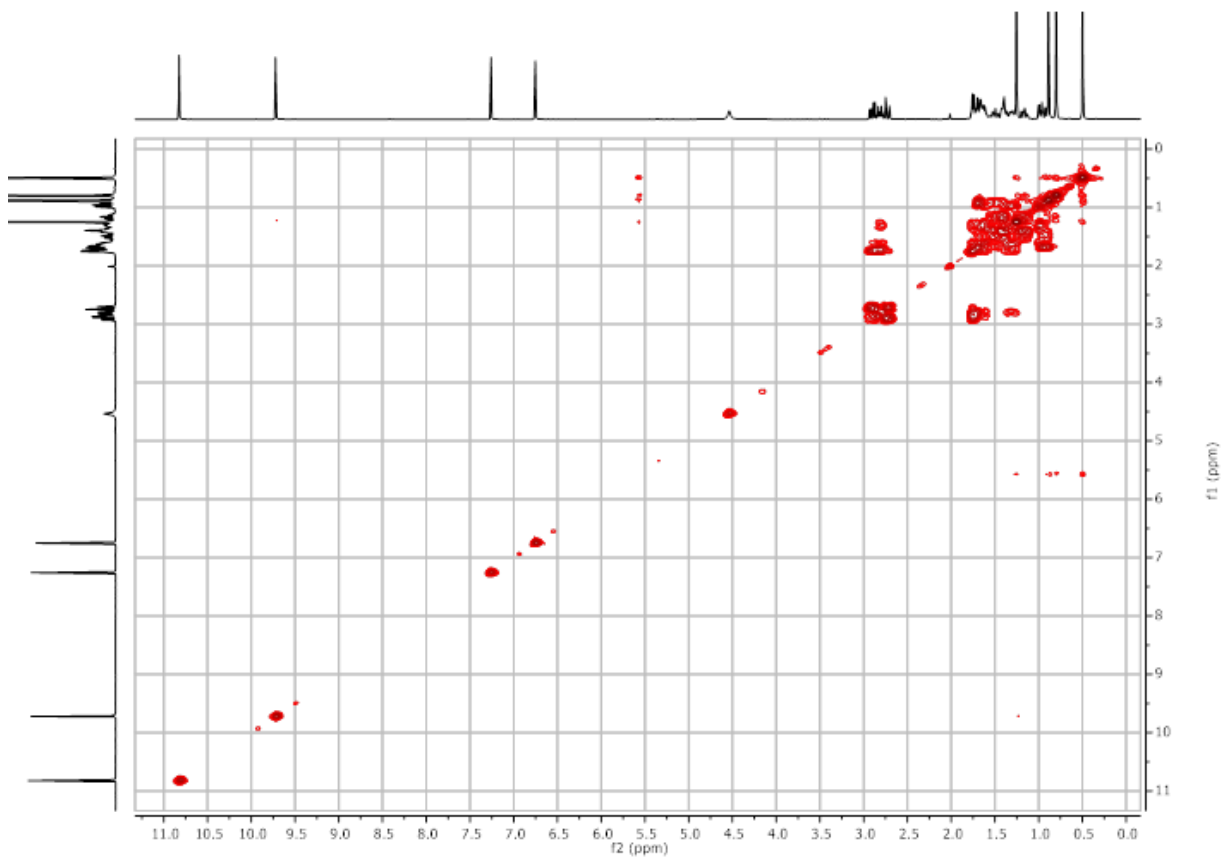


Figure 6. COSY NMR Spectrum of **1**.

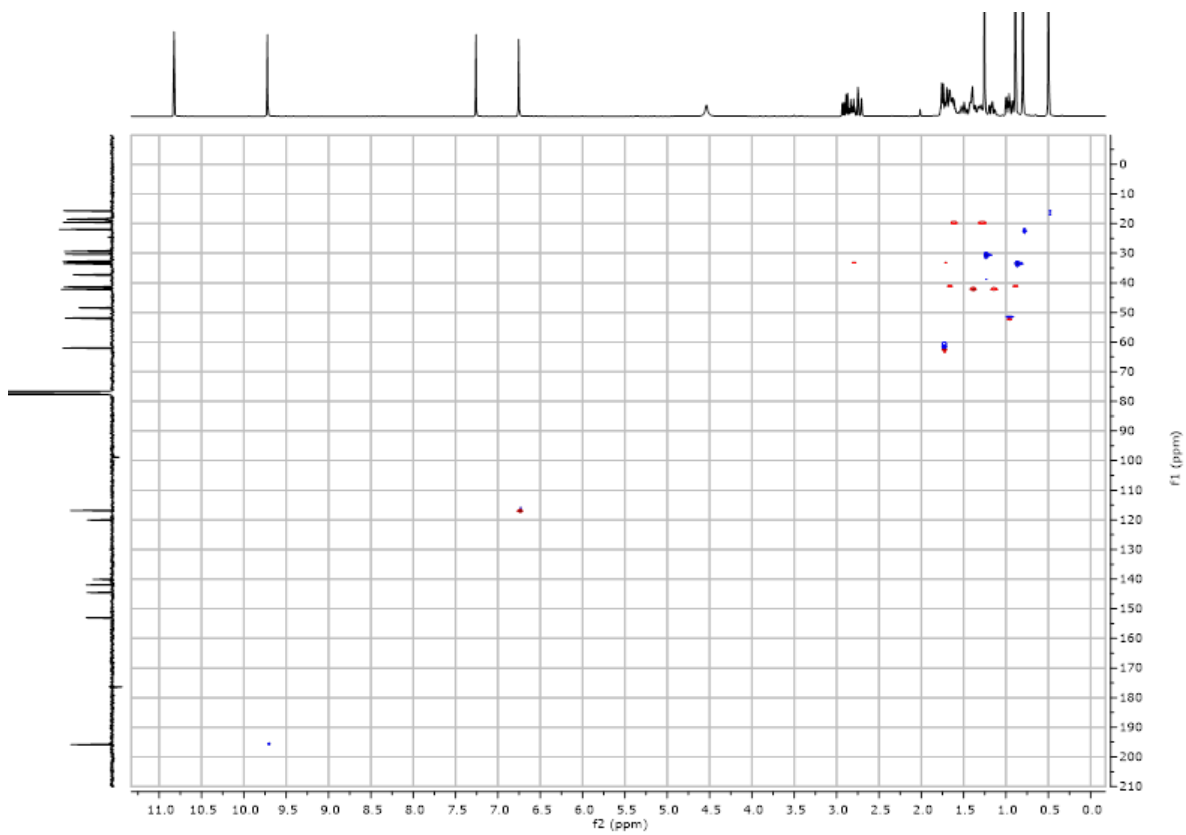


Figure 7. HSQC NMR Spectrum of **1**.

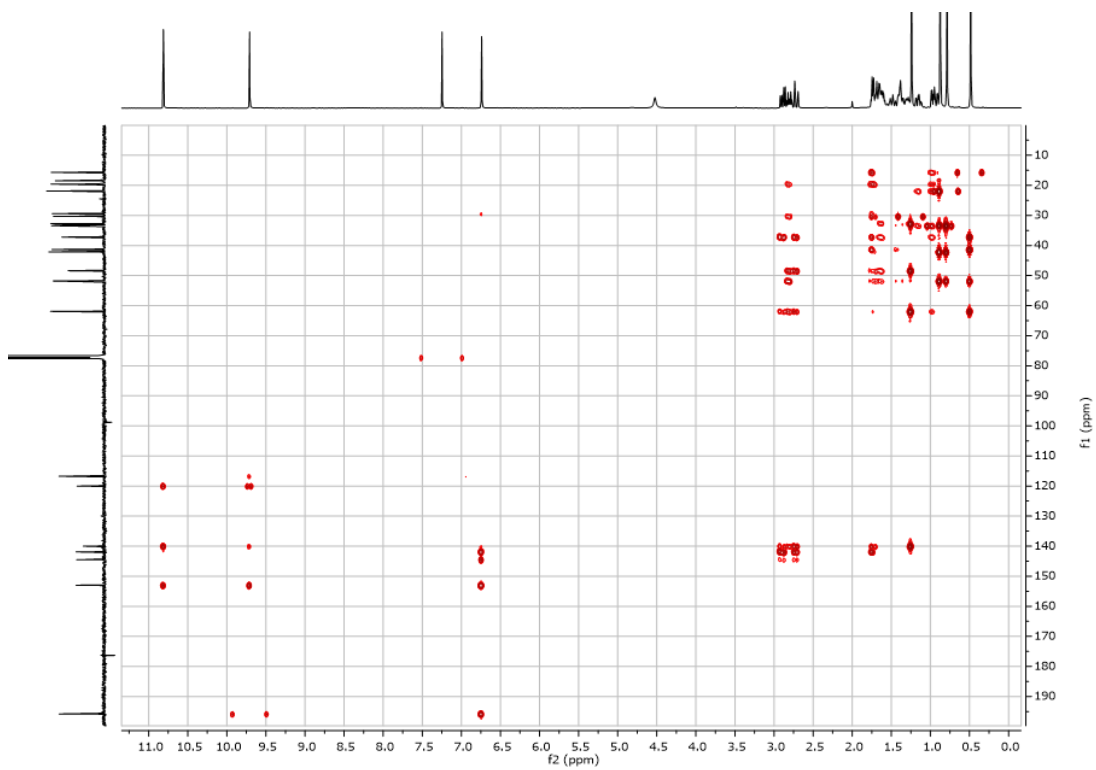


Figure 8. HMBC NMR Spectrum of **1**.

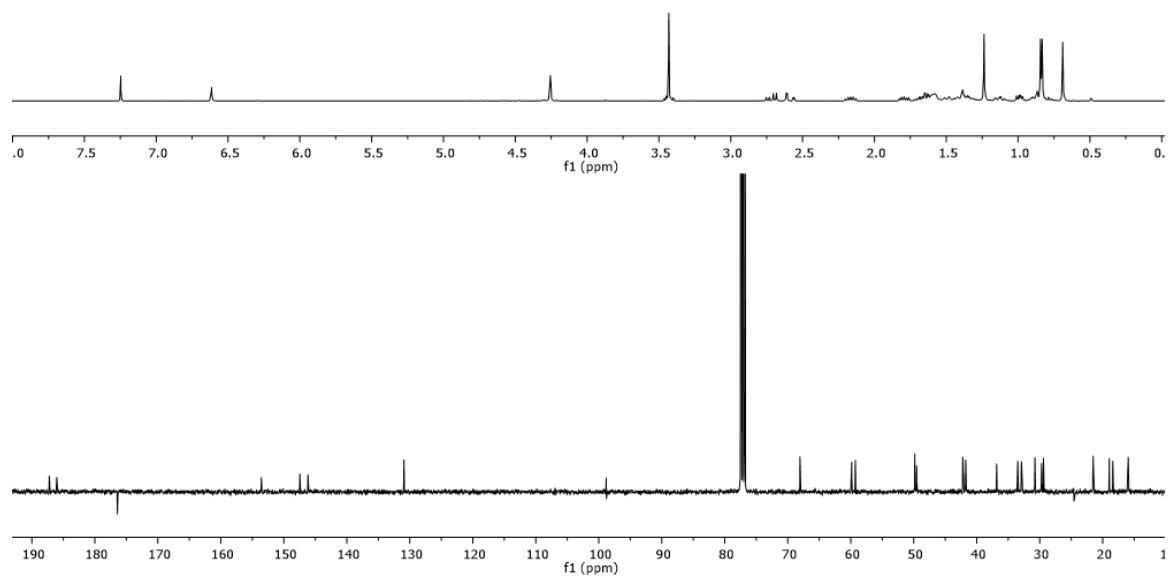


Figure 9. ^1H and ^{13}C NMR Spectra of **2**.

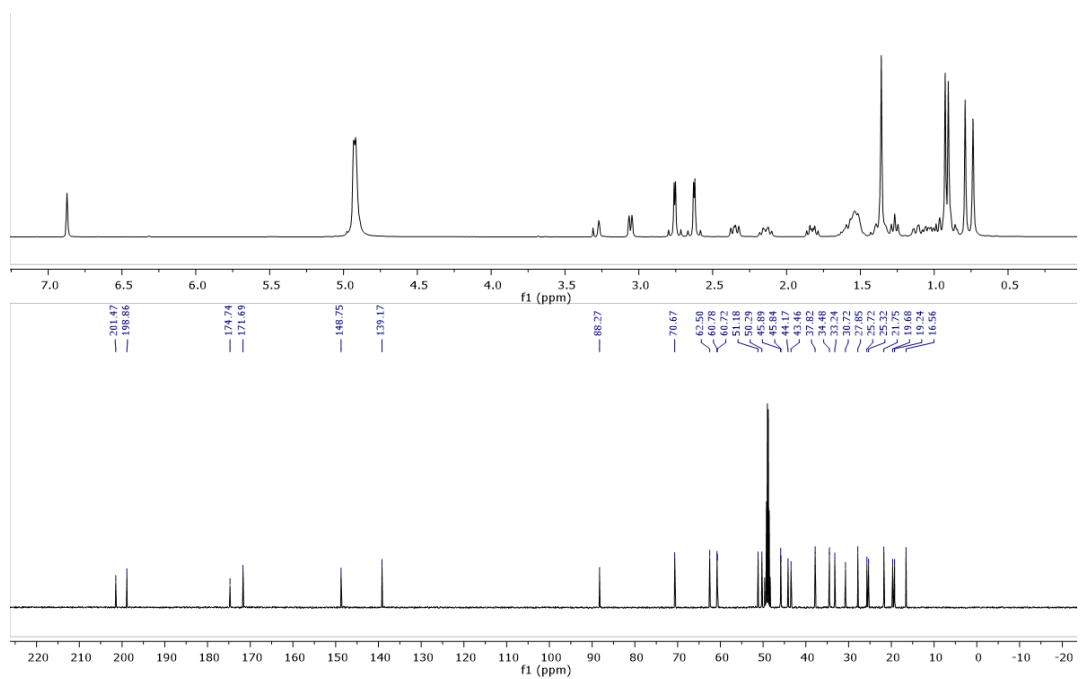


Figure 10. ^1H and ^{13}C NMR Spectra of **3**.